Defect Engineering within Transition Metal Dichalcogenides and Machine Learning Approaches towards STM/STS Tip Shaping on Au

John C. Thomas, Katherine A. Cochrane, Alexander Weber-Bargioni
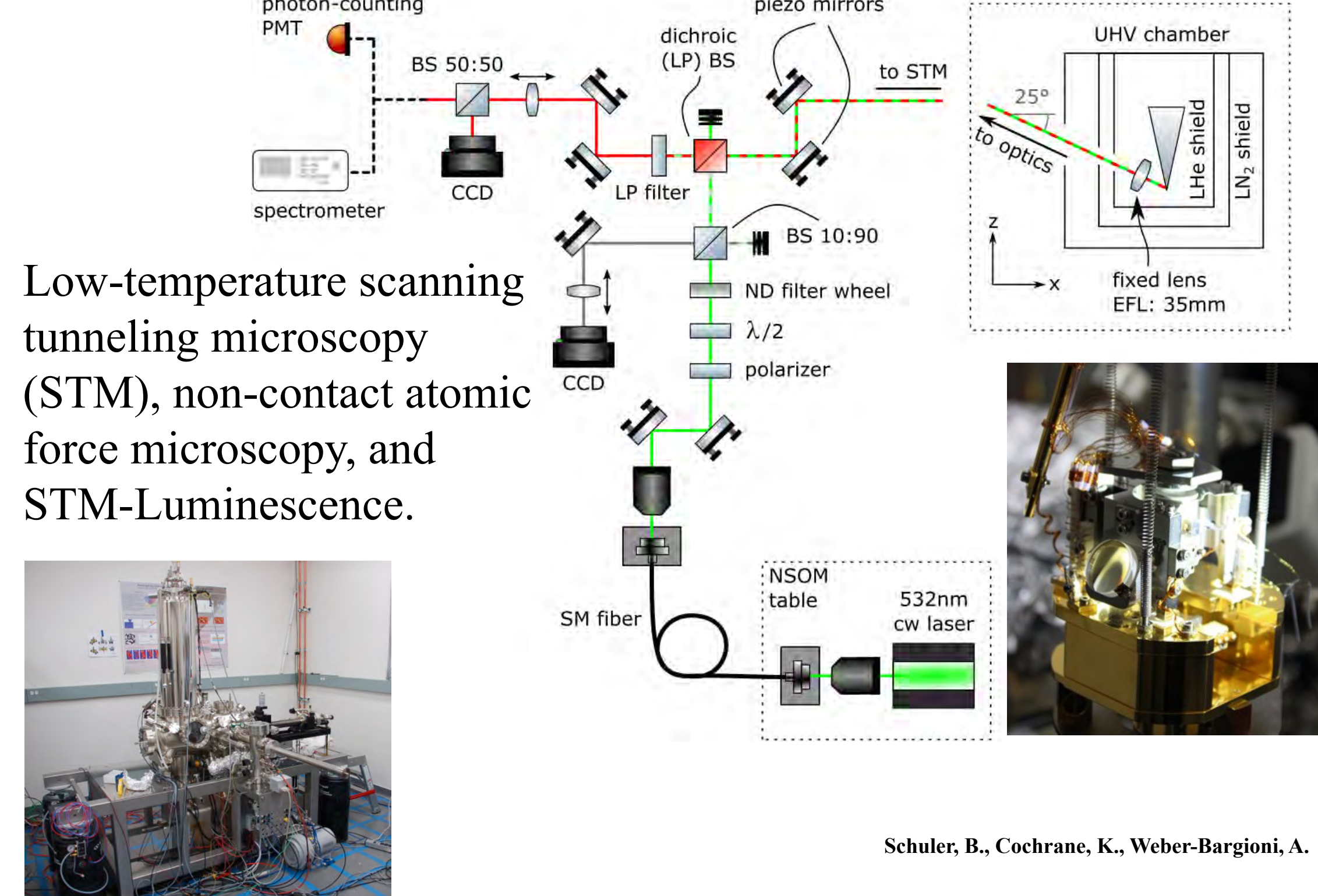Lawrence Berkeley National Laboratory

Transition Metal Dichalcogenides

Monolayer systems that interact via van der Waals forces, with the formula MX_2, are bound to a semiconducting substrate encapsulated with graphene.

Here, the indirect (bulk TMD) to direct band gap (monolayer TMD) can be observed.

TMD heterostructures combined with defect control enable access to tunable electronic or optoelectronic properties by modulating defective regions, strain induced states, and dielectric modification.

Locally confined sheets are susceptible to defect creation and subsequent functionalization.

Experiment

Low-temperature scanning tunneling microscopy (STM), non-contact atomic force microscopy, and STM-Luminescence.

Schuler, B., Cochrane, K., Weber-Bargioni, A.

Automation

Machine learning (ML) techniques are combined with the Nanonis programming interface to direct and control tip-shaping protocols. The tool is directed to acquire an image over Au(111) that is fed into an ML classifier: if an image is deemed of high enough quality the tip is retracted for the user, if the area is over a step or multi-step edge the tip is moved until a flat terrace is found, or the tip undergoes tip-shaping and the loop is repeated.
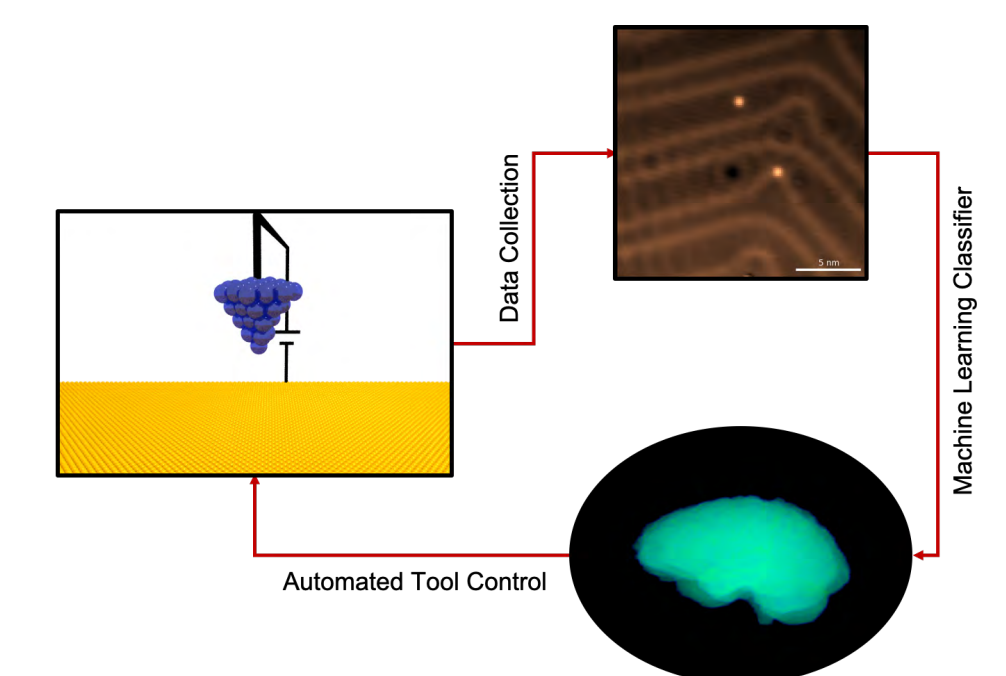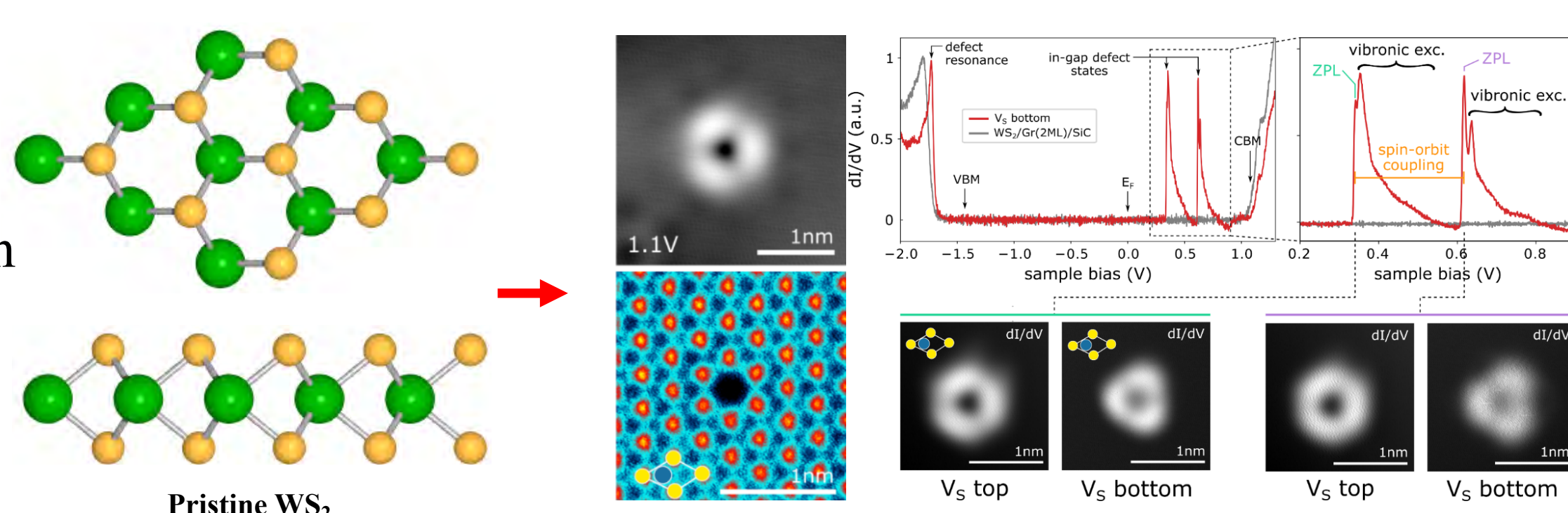

Tungsten Disulfide Defect Creation

SPM enables layer identification at the atomic scale.
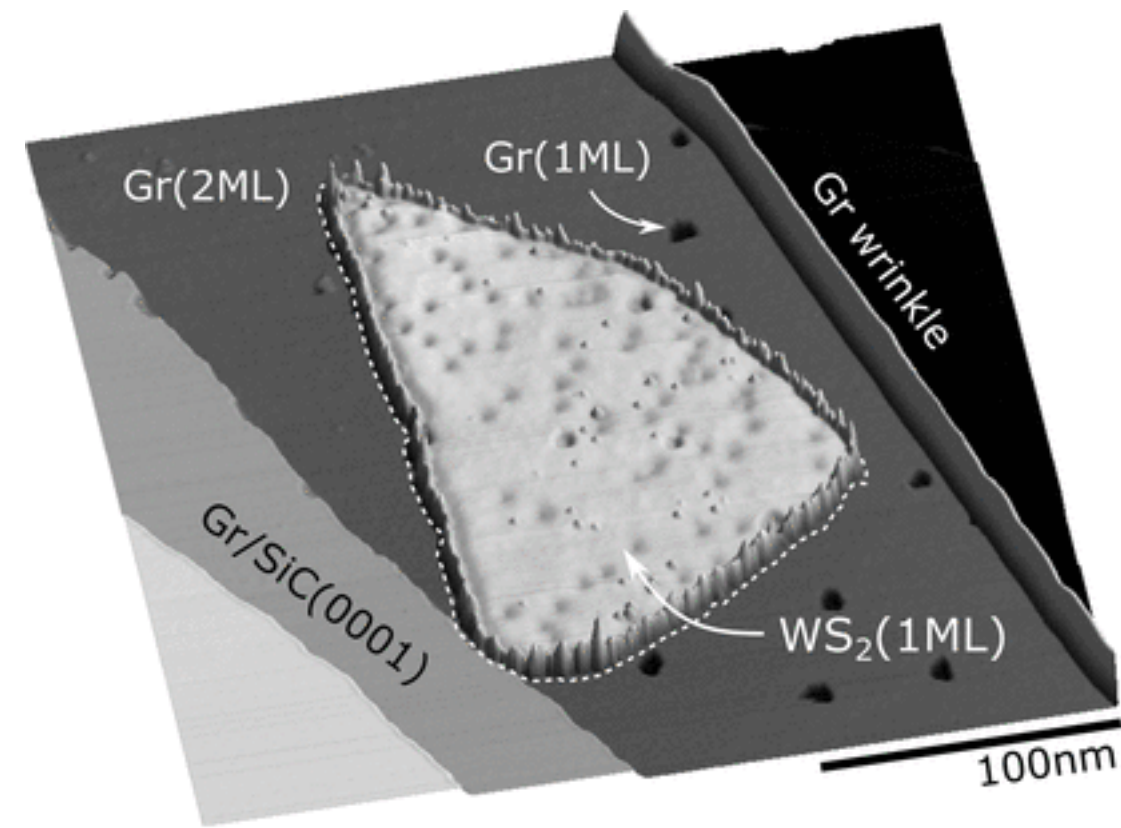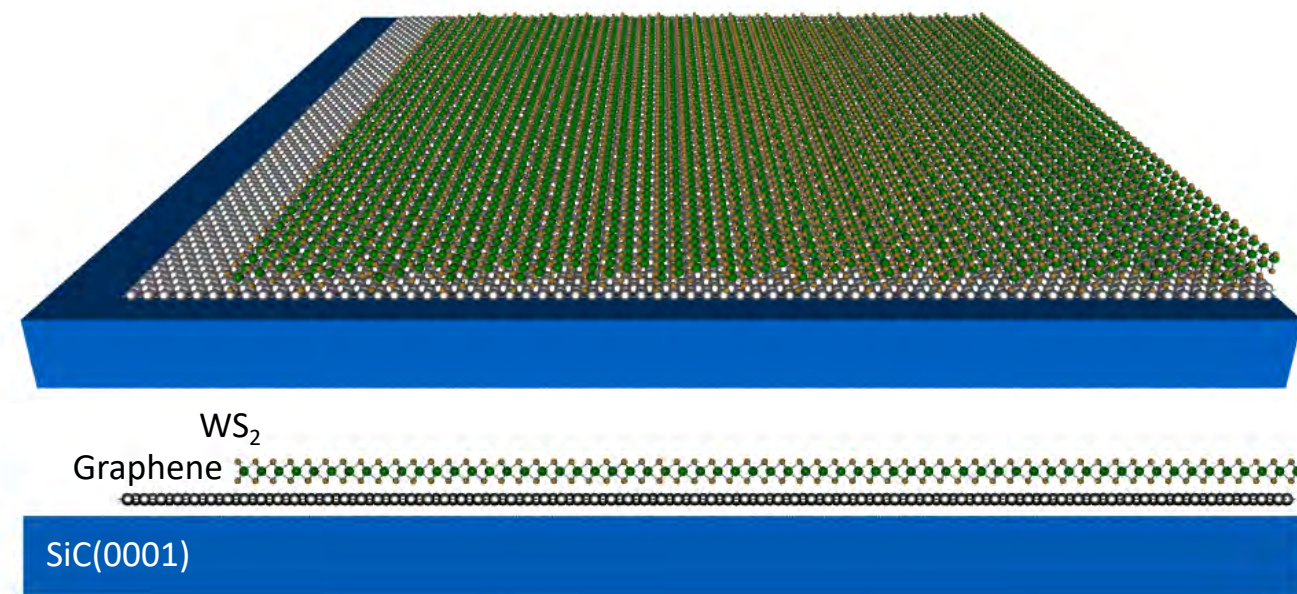
WS_2 sulfur vacancies are generated by annealing at 600 °C for 30 minutes. Defects can then be identified and characterized for subsequent functionalization.

Pristine WS_2

A dual sample holder is used to verify metal deposition on Au(111) before measuring TMD. A custom-built evaporator that holds Co is brought near the sample held at 4 K for low-temperature deposition.
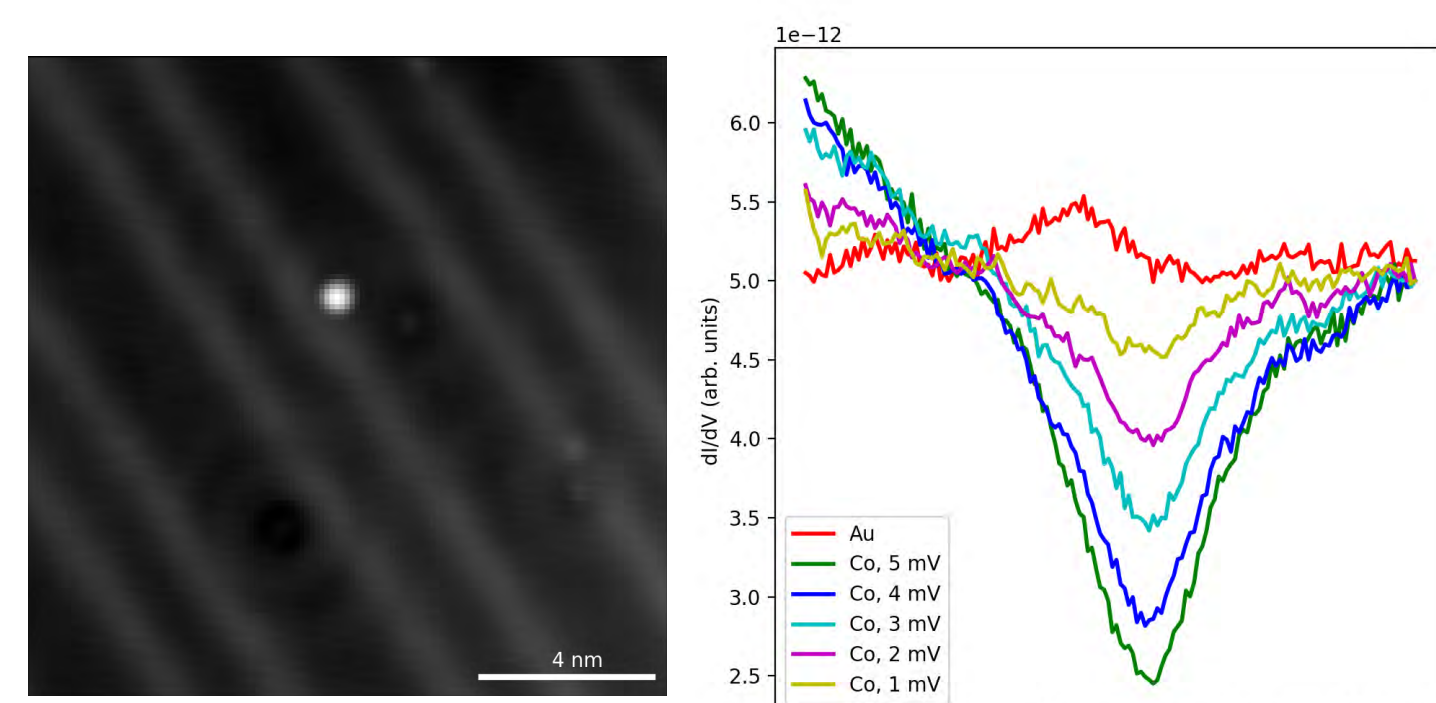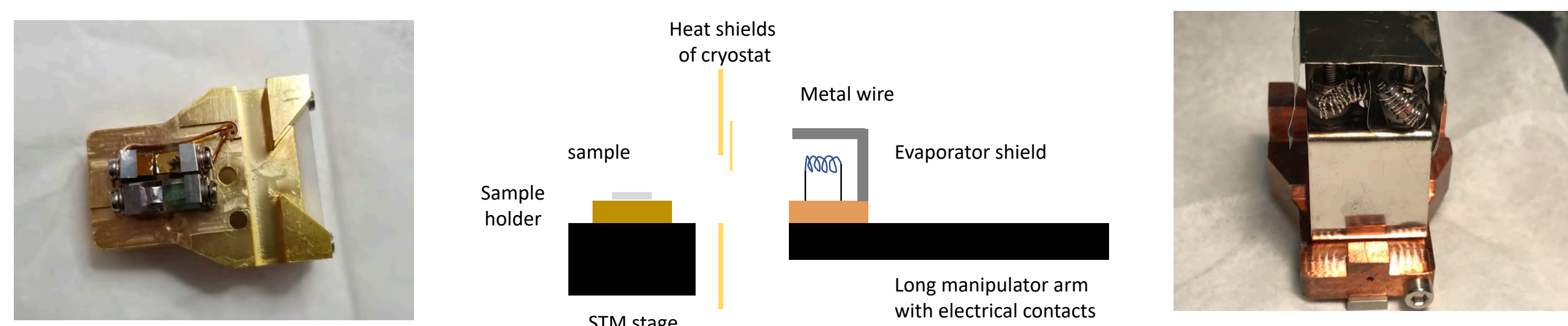
Defect Creation in 2D Materials

Defects are created as expected with high temperature in vacuum.
- Local information is obtained via multi-modal SPM combined with STS.

Automated Tip-Shaping

Double-, or multi-, tips are a common problem for scanning probe systems.

Chen et al., J. Surf. Eng. Mater. Adv. Technol. **2**, 238 (2012)

Schema:
Compute the 2D discrete Fourier Transform. Solve for local maxima within a given pixel window above a given threshold (mean of z data).
Compute number of maxima, angle between maxima with respect to image center in different quadrants, compute pixel distance, and compute FFT pixel entropy.

$$-\sum_{j=1} p_j log_2(p_j)$$
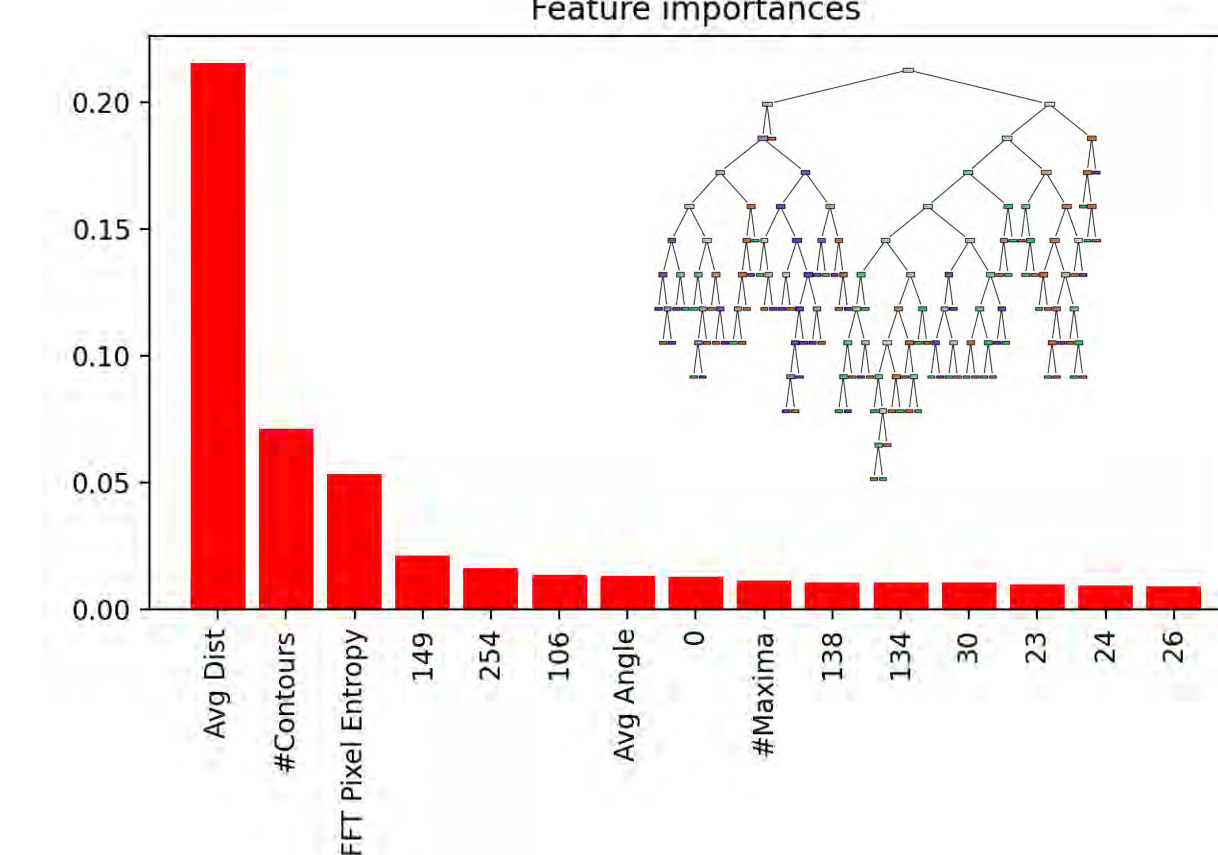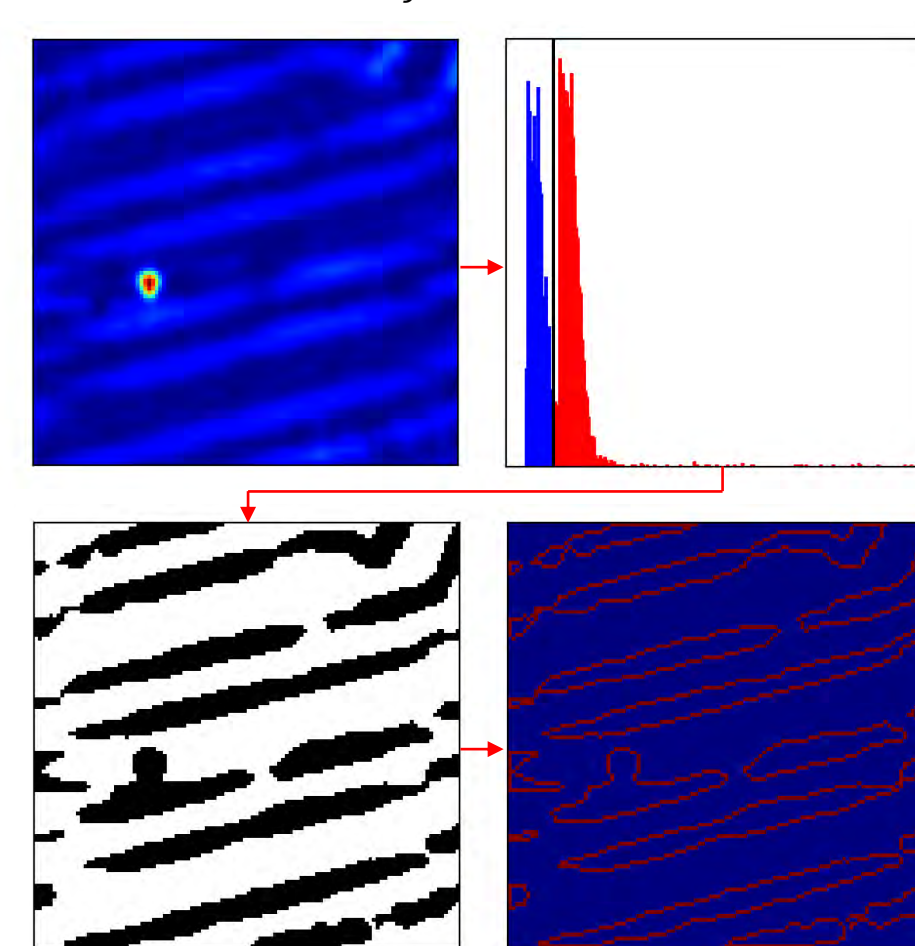
Features are extracted from each image to feed into a random forest classifier for training.
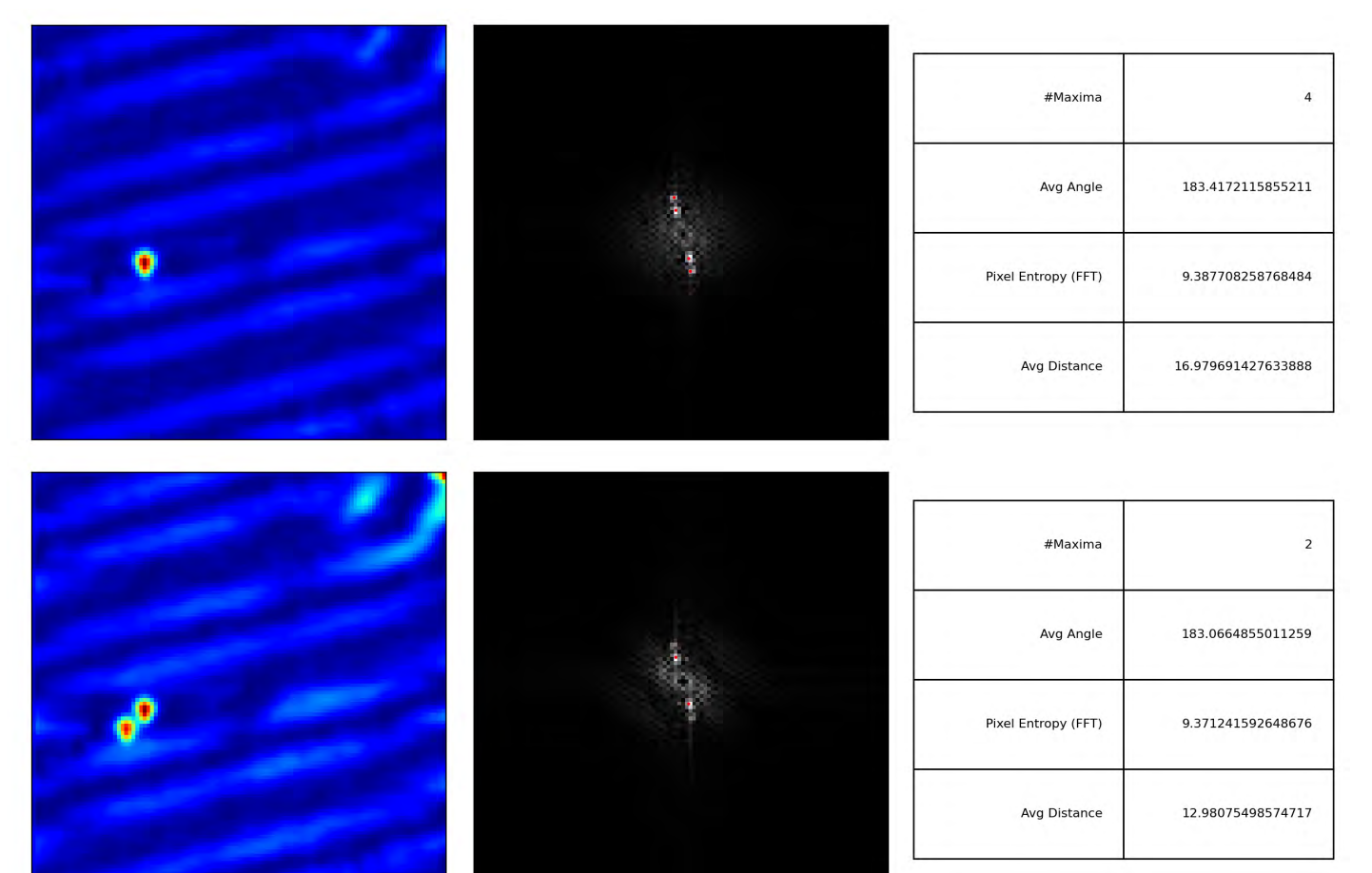
Otsu's method is chosen as an automatic method, where a threshold value is determined by variation optimization.
A border following algorithm (useful in topological structure) then detects the number of borders (between 0 and 1 pixels) and solves for the the parent border, which gives the number of contours in each thresholded image.

Suzuki et al., Comput. Gr. Image Process. **30**, 32 (1985)
Digital Image Processing, Rafael C. Gonzalez

Feature importances

A dataset of over 3000 images is used and subsequent double or multi-tip images are generated. Importances indicate the predominant features contributing to classification using an entropy minimized RFC that obtains a 90 % accuracy score on test data after sufficient training.

RFC is computationally less expensive compared with a convolutional neural network and achieves comparable accuracy on herringbone-resolved vs atomically-resolved gold images.
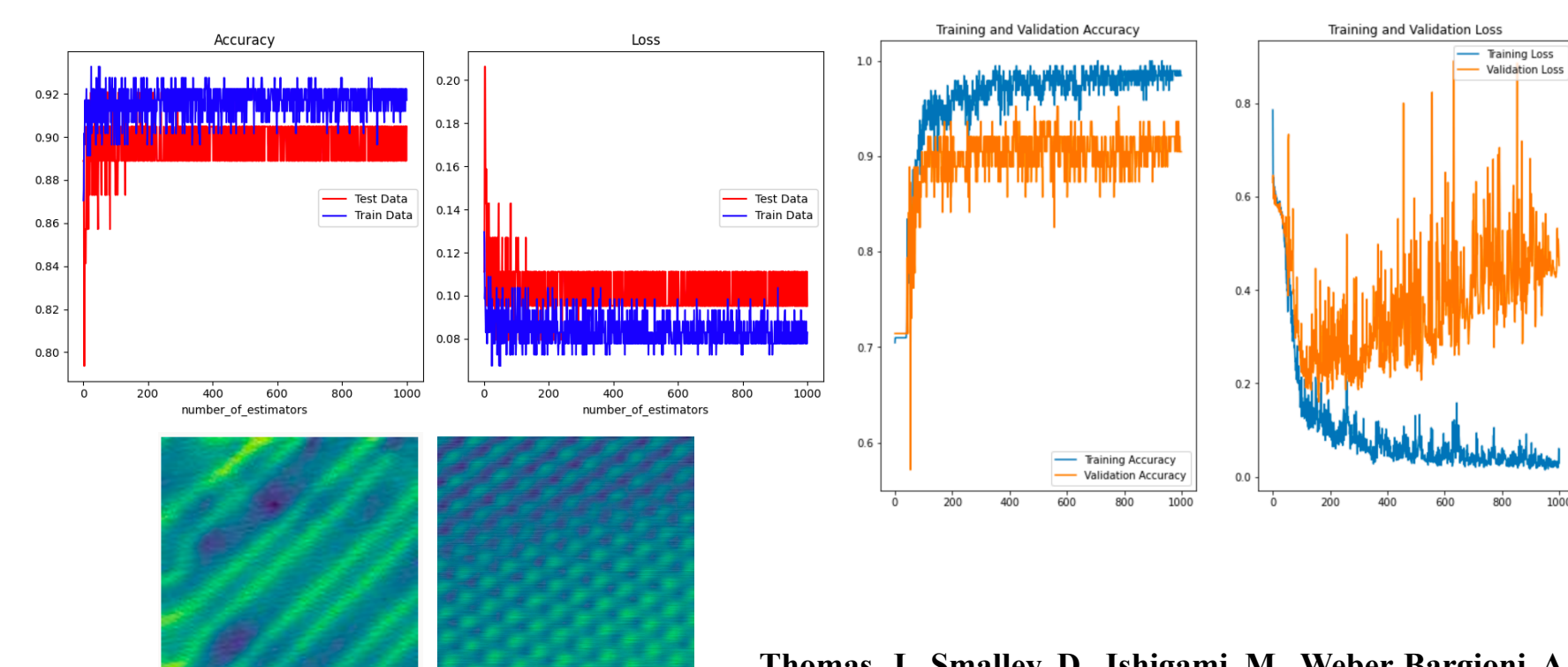
Thomas, J., Smalley, D., Ishigami, M., Weber-Bargioni, A.

Machine Learning Techniques

Au regions are identified with artificial intelligence classifiers using a supervised learning approach.
- Tip-shaping can then be automated after acquired data is classified for both imaging and spectroscopy.

1. Schuler, B.; Cochrane, K. A.; Kastl, C.; Barnard, E. S.; Wong, E.; Borys, N. J.; Schwartzberg, A. M.; Ogletree, D. F.; de Abajo, F. J. G.; Weber-Bargioni, A. Sci. Adv. **6**, (2020).
2. Cochrane, K. A.; Lee, J.; Kastl, C.; Haber, J. B.; Zhang, T.; Kozhakhmetov, A.; Robinson, J. A.; Terrones, M.; Repp, J.; Neaton, J. B.; Weber-Bargioni, A.; Schuler, B. arXiv2008.12196r (2020).
3. Cochrane, K. A.; Zhang, T; Kozhakhmetov, A.; Lee, J.; Zhang, F.; Dong, C.; Neaton, J. B.; Robinson, J. A.; Terrones, M.; Weber-Bargioni, A.; Schuler, B. 2D Mater. **7**, 031003 (2020).
4. Schuler, B.; Qiu, D. Y.; Refaely-Abramson, S.; Kastl, C.; Chen, C. T.; Barja, S.; Koch, R. J.; Ogletree, D. F.; Aloni, S.; Schwartzberg, A. M.; Neaton, J. B.; Louie, S. G.; Weber-Bargioni, A. Phys. Rev. Lett. **123**, 076801 (2019).
5. Schuler, B.; Lee, J.; Kastl, C.; Cochrane, K. A.; Chen, C. T.; Refaely-Abramson, S.; Yuan, S.; van Veen, E.; Roldán, R.; Borys, N. J.; Koch, R. J.; Aloni, S.; Schwartzberg, A. M.; Ogletree, D. F.; Neaton, J. B.; Weber-Bargioni, A. ACS Nano **13**, 10520-10534 (2019)